Title

Climate Change in the South American Monsoon System: Present Climate and CMIP5 Projections

Journal

Journal of Climate, 26(17)

ISSN

0894-8755 1520-0442

Authors

Jones, Charles
Carvalho, Leila M. V

Publication Date

2013-09-01

DOI

10.1175/JCLI-D-12-00412.1

Peer reviewed

Climate Change in the South American Monsoon System: Present Climate and CMIP5 Projections

CHARLES JONES

Earth Research Institute, University of California, Santa Barbara, Santa Barbara, California

LEILA M. V. CARVALHO

Earth Research Institute, and Department of Geography, University of California, Santa Barbara, Santa Barbara, California

(Manuscript received 6 July 2012, in final form 1 March 2013)

ABSTRACT

The South American monsoon system (SAMS) is the most important climatic feature in South America. This study focuses on the large-scale characteristics of the SAMS: seasonal amplitudes, onset and demise dates, and durations. Changes in the SAMS are investigated with the gridded precipitation, Climate Forecast System Reanalysis (CFSR), and the fifth phase of the Coupled Model Intercomparison Project (CMIP5) simulations for two scenarios [''historical'' and high-emission representative concentration pathways (rcp8.5)]. Qualitative comparisons with a previous study indicate that some CMIP5 models have significantly improved their representation of the SAMS relative to their CMIP3 versions. Some models exhibit persistent deficiencies in simulating the SAMS. CMIP5 model simulations for the historical experiment show signals of climate change in South America. While the observational data show trends, the period used is too short for final conclusions concerning climate change. Future changes in the SAMS are analyzed with six CMIP5 model simulations of the rcp8.5 high-emission scenario. Most of the simulations show significant increases in seasonal amplitudes, early onsets, late demises, and durations of the SAMS. The simulations for this scenario project a 30% increase in the amplitude from the current level by 2045–50. In addition, the rcp8.5 scenario projects an ensemble mean decrease of 14 days in the onset and 17-day increase in the demise date of the SAMS by 2045–50. The results additionally indicate lack of spatial agreement in model projections of changes in total wet-season precipitation over South America during 2070–2100. The most consistent CMIP5 projections analyzed here are the increase in the total monsoon precipitation over southern Brazil, Uruguay, and northern Argentina.

1. Introduction

Observational and theoretical evidence points to the undeniable fact that Earth's climate is changing rapidly and anthropogenic activities play a vital role (Solomon et al. 2007; Field et al. 2012). In preparation for the next assessment of the Intergovernmental Panel on Climate Change (IPCC), the fifth phase of the Coupled Model Intercomparison Project (CMIP5) has coordinated a large set of experiments to evaluate climate model performance, explore decadal climate predictability, and investigate differences in multimodel climate projections (Taylor et al. 2012). Capitalizing on this research effort, the goal of this paper is to document changes in large-scale characteristics of the monsoon in South America [hereafter, the South American monsoon system (SAMS)] in reanalysis, precipitation, and CMIP5 model simulations.

The SAMS is the most important climatic feature in South America (Kousky 1988; Horel et al. 1989; Zhou and Lau 1998; Vera et al. 2006b; Marengo et al. 2012) and provides water resources for the millions of people living in the continent (e.g., Berbery and Barros 2002; Grimm 2011; Jones et al. 2012). Documenting climate change in South America is necessary to motivate additional studies to further understand potential impacts on environment, societies, and economies.

The main feature of the SAMS is the enhanced convective activity and heavy precipitation in tropical South America, which typically starts in October–November

Corresponding author address: Dr. Charles Jones, Earth Research Institute, University of California, Santa Barbara, Santa Barbara, CA 93106.
E-mail: cjones@eri.ucsb.edu

DOI: 10.1175/JCLI-D-12-00412.1

and is fully developed during December–February and retreats in late April or early May (Kousky 1988; Horel et al. 1989; Marengo et al. 2001; Grimm et al. 2005; Gan et al. 2006; Liebmann et al. 2007; Silva and Carvalho 2007). Associated with intense latent heat release in the region of heavy precipitation, the large-scale atmospheric circulation is characterized by the upper-level ''Bolivian high'' and ''Nordeste'' trough, the ''Chaco'' surface low-pressure low-level jet east of the Andes (Silva Dias et al. 1983; Gandu and Silva Dias 1998; Lenters and Cook 1999; Marengo et al. 2002), and the South Atlantic convergence zone (SACZ) (Kodama 1992, 1993; Carvalho et al. 2004).

The SAMS has been the subject of several studies that demonstrated important types of variability on diurnal, synoptic, intraseasonal, seasonal, interannual, and decadal time scales (Hartmann and Recker 1986; Robertson and Mechoso 1998; Liebmann et al. 1999; Robertson and Mechoso 2000; Liebmann et al. 2001; Carvalho et al. 2002b; Jones and Carvalho 2002; Grimm 2003; Carvalho et al. 2004; Grimm 2004; Liebmann et al. 2004a; Marengo 2004; Grimm and Zilli 2009; Marengo 2009; Carvalho et al. 2011a,b). The spatial extent and timing of the wet-season precipitation varies significantly over South America (Berbery and Collini 2000; Carvalho et al. 2002a; Durieux et al. 2003; Bookhagen and Strecker 2008; Marengo et al. 2012) and large changes in precipitation have dramatic impacts on hydropower generation and water resources in urban regions (Mechoso et al. 2005; Marengo et al. 2011).

Climate change has motivated several studies to investigate possible impacts over South America. Vera et al. (2006a) analyzed a subset of the third phase of the Coupled Model Intercomparison Project (CMIP3) simulations that contributed to the fourth assessment of the IPCC. They conclude that those models are able to simulate the observed climatological seasonal precipitation over South America, although deficiencies are noted in simulating precipitation over the SACZ and cold-season precipitation maximum over southeastern South America. In addition, the results for one particular scenario suggest an increase in summer precipitation over southeastern subtropical South America and reduction in continental winter precipitation. Using a regional climate model to analyze changes in temperature and precipitation under two CMIP3 scenarios, Marengo et al. (2009) found evidence of increase in the frequency of warm nights over tropical South America, decrease in cold nights, and increased intensity of extreme precipitation over southeastern South America and western Amazonia. Seth et al. (2010) also analyzed CMIP3 multimodel simulations for one climate change scenario and suggested an increase in warm season precipitation over southeastern South America, particularly over the SACZ. Kitoh et al. (2011) carried out ensemble simulations with a high-resolution global atmospheric model and found an increase in wet-season precipitation and a decrease in dry-season precipitation over most of South America. Their results also suggest that changes in precipitation patterns are likely to increase extreme precipitation over southeast South America and increase in the frequency of dry days over the western Amazon. In another study, Seth et al. (2011) found that CMIP3 climate model projections suggest a redistribution of precipitation from spring to summer in northern (North America, West Africa, and Southeast Asia) and southern (South America and southern Africa) regions.

While the studies above show some consistent features, large uncertainties exist in regional climate change over South America as simulated by CMIP3 models. Bombardi and Carvalho (2009) analyzed 10 CMIP3 models for the present and one future climate scenario. They conclude that most models misrepresent the intertropical convergence zone (ITCZ) and the annual cycle of precipitation over the Amazon and northwest South America. CMIP3 models correctly represent the spatiotemporal variability of the annual cycle of precipitation in central and eastern Brazil including the phase of dry and wet seasons, onset dates, duration of rainy season, and total accumulated precipitation during the SAMS. Most CMIP3 models, however, misrepresent the total monsoonal precipitation over the Amazon and northeast Brazil. Their results suggest a reduction in precipitation over central-eastern Brazil during the summer monsoon and no statistically significant changes in onset and demise dates of the SAMS during the A1B climate change scenario.

Motivated by the availability of CMIP5 model simulations, this study documents changes in the SAMS. The paper specifically focuses on the large-scale characteristics of the SAMS: seasonal amplitudes, onset and demise dates, and duration. The following questions are investigated: 1) Are there significant trends in the large-scale characteristics of the SAMS? 2) Do CMIP5 climate models realistically simulate the observed characteristics of the SAMS? 3) Do CMIP5 models project significant changes in the large-scale characteristics of the SAMS during the twenty-first century? These questions are investigated with observed gridded precipitation, reanalysis, and CMIP5 model simulations for two scenarios (section 2). We first define and discuss the large-scale characteristics of the SAMS during 1979–2010 (section 3). Next, the performance of CMIP5 models in simulating the large-scale characteristics of the SAMS are analyzed (section 4). CMIP5 projections of changes

TABLE 1. List of CMIP5 models used in this study and complete model expansions. All 10 models are used for analyses of the historical experiment.

	Modeling center (or group)	Institute ID	Model name	Model abbreviation
1	Canadian Centre for Climate Modeling and Analysis	CCCMA	Second Generation Canadian Earth System Model	CanESM2*
2	Centre National de Recherches Meteorologiques–Centre Europeen de Recherche et Formation Avancees en Calcul Scientifique	CNRM–CERFACS	Centre National de Recherches Météorologiques Coupled Global Climate Model, version 5	CNRM-CM5
3	Commonwealth Scientific and Industrial Research Organization in collaboration with Queensland Climate Change Centre of Excellence	CSIRO–QCCCE	Commonwealth Scientific and Industrial Research Organisation Mark, version 3.6.0	CSIRO-Mk3.6.0
4	National Oceanic and Atmospheric Administration (NOAA) Geophysical Fluid Dynamics Laboratory	NOAA GFDL	Geophysical Fluid Dynamics Laboratory Earth System Model with MOM4 ocean component	GFDL-ESM2M*
5	Institute for Numerical Mathematics	INM	Institute of Numerical Mathematics Coupled Model, version 4.0	INM-CM4
6	Institut Pierre-Simon Laplace	IPSL	Institute of Numerical Mathematics Coupled Model, version 4.0	IPSL-CM5A-LR
7	Atmosphere and Ocean Research Institute (The University of Tokyo), National Institute for Environmental Studies, and Japan Agency for Marine-Earth Science and Technology	MIROC	Model for Interdisciplinary Research on Climate, version 4 (high resolution)	MIROC4h
			Model for Interdisciplinary Research on Climate, version 5	MIROC5*
8	Max Planck Institute for Meteorology	MPI-M	Max Planck Institute Earth System Model, low resolution	MPI-ESM-LR*
9	Meteorological Research Institute	MRI	Meteorological Research Institute Coupled Atmosphere–Ocean General Circulation Model, version 3	MRI-CGCM3*
10	Norwegian Climate Centre	NCC	Norwegian Earth System Model, version 1 (medium resolution)	NorESM1-M*

* Indicates models analyzed for the rcp8.5 scenario.

in the SAMS for one climate change scenario are analyzed (section 5) and summary and conclusions are presented (section 6).

2. Data

Precipitation (PREC) over South America is characterized with the gridded Climate Prediction Center unified gauge (CPCU) data. CPCU uses an optimal interpolation technique to reproject precipitation reports to a grid (Higgins et al. 2000; Silva et al. 2007; Chen et al. 2008; Silva et al. 2011). This study uses daily data with 0.5° latitude/longitude grid spacing during 1979–2010. Since CPCU is available only over land, Tropical Rainfall Measurement Mission (TRMM 3B42V6) data (Kummerow et al. 1998; Kummerow et al. 2000; Huffman et al. 2007; Bookhagen and Burbank 2010) are additionally used to evaluate the performance of CMIP5 models in simulating climatological features over South America and the Atlantic Ocean. This study uses TRMM data degraded to 0.5° latitude/longitude grid spacing and available during 1998–2010.

The large-scale features of the SAMS are characterized with the National Centers for Environmental Prediction (NCEP) Climate Forecast System Reanalysis (CFSR; Saha et al. 2010) at 0.5° latitude/longitude grid spacing from 1 January 1979 to 31 December 2010. Daily averages of the zonal (U850) and meridional (V850) components of the wind, specific humidity (Q850), and temperature (T850) at 850 hPa are used. The advantages of CFSR relative to the previous NCEP reanalysis include high horizontal and vertical resolutions, improvements in data assimilation, and first-guess fields originated from a coupled atmosphere–land–ocean–ice system (Higgins et al. 2010; Saha et al. 2010).

Changes in the SAMS are investigated with multimodel ensemble from the fifth phase of the Coupled Model Intercomparison Project (Taylor et al. 2012). Model simulations from CMIP5 provide the basis for the Fifth Assessment Report (AR5) of the Intergovernmental Panel on Climate Change. Additional information about CMIP5 can be found online at http://cmip-pcmdi.llnl.gov/cmip5/.

The following model experiments are analyzed to investigate long-term changes in the SAMS. The ''historical'' run (also known as the ''twentieth-century simulation'') was forced by observed atmospheric composition changes which include both anthropogenic and natural sources as well as time-evolving land cover. The historical run covers the period from 1 January 1951 to 31 December 2005. In addition, CMIP5 simulations of climate projection are forced with specified concentrations referred to as ''representative concentration pathways'' (RCPs) and provide a rough estimate of the radiative forcing in the year 2100 relative to preindustrial conditions (Moss et al. 2010; Taylor et al. 2012). To investigate future changes in the SAMS, the ''high-emission'' scenario labeled as ''rcp8.5'' is used. In this scenario, radiative forcing increases throughout the twenty-first century before reaching a level of $\sim 8.5\ \mathrm{W\ m^{-2}}$ at the end of the century. Rcp8.5 simulations cover the period from 1 January 2006 to 31 December 2100. Although other scenarios are available in CMIP5, rcp8.5 is used here to examine potentially large changes in the SAMS.

Table 1 alphabetically lists the models and all model expansions used in this study. The analysis of the historical experiment includes all 10 models. Because of difficulties in accessing CMIP5 data, however, only the following models were analyzed for the rcp8.5 scenario: CanESM2, GFDL-ESM2M, MIROC5, MPI-ESM-LR, MRI-CGCM3, and NorESM1-M. Given the large volume of data, only one run from each model and experiment was used in this study. Although more models are available in CMIP5, at the time this work was conducted daily outputs were available only for the models listed in Table 1.

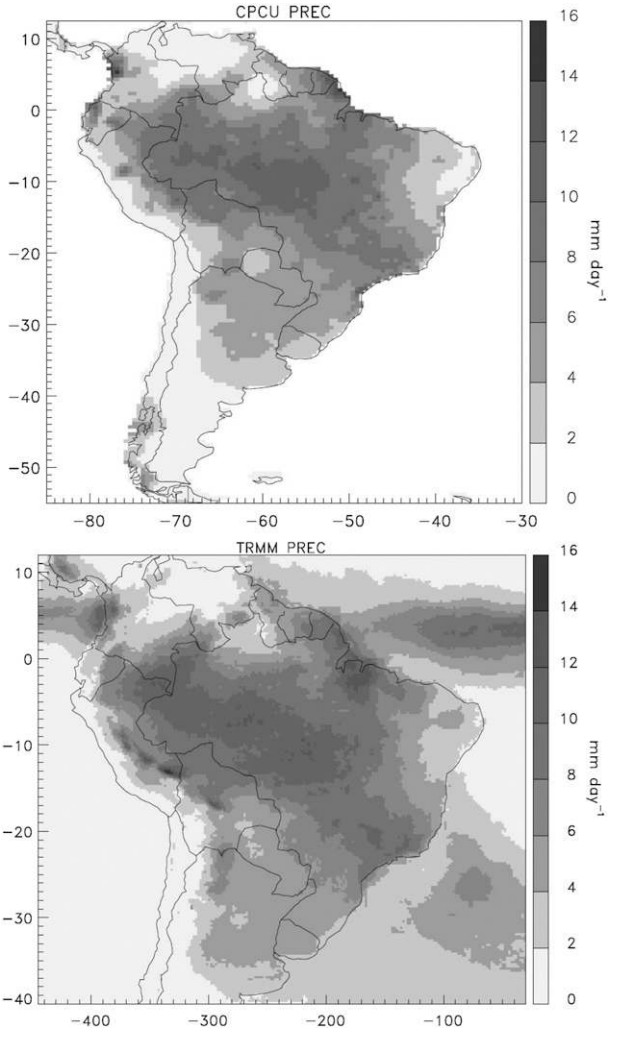

FIG. 1. Mean precipitation during December–February (mm day^{-1}). (top) CPC-unified gridded data (1979–2010) and (bottom) TRMM data (1998–2010).

3. Changes in large-scale characteristics of the SAMS: Observations

The wet season is a major climatological feature in South America (Kousky 1988; Horel et al. 1989; Liebmann et al. 2007). Furthermore, the atmospheric circulation exhibits pronounced changes coupled to the region of intense latent heat release. The mean precipitation during the peak of the monsoon season (December–February; Fig. 1) maximizes over the Amazon basin and extends toward southeast Brazil. It is interesting to note that another maximum is observed over the oceanic portion of the SACZ (Carvalho et al. 2002a, 2004); another feature not represented in the CPCU data but well captured by TRMM is the intertropical convergence zone (Fig. 1b). The representation of the summer climatology by the CMIP5 models is discussed in section 4.

To characterize the amplitude, onset, demise, and duration of the monsoon, we employ the large-scale index for the South American monsoon (LISAM) developed by Silva and Carvalho (2007). LISAM is based on combined empirical orthogonal function (EOF) analysis (Wilks 2006) of PREC, U850, V850, Q850, and T850. Since LISAM is calculated with gridded fields, it is a useful methodology to evaluate the skill of climate models in simulating the SAMS.

Each field is scaled by the square root of the cosine of the latitude and only the long-term mean (1979–2010) is subtracted from each field prior to the calculation of EOF. The first mode (EOF1) accounts for 19.3% of the total variance (Fig. 2). Maximum precipitation variability is observed over parts of the Amazon and central Brazil. Easterly anomalies are observed over the equatorial Atlantic and subtropics, whereas westerly anomalies are noted over most of tropical South America. The

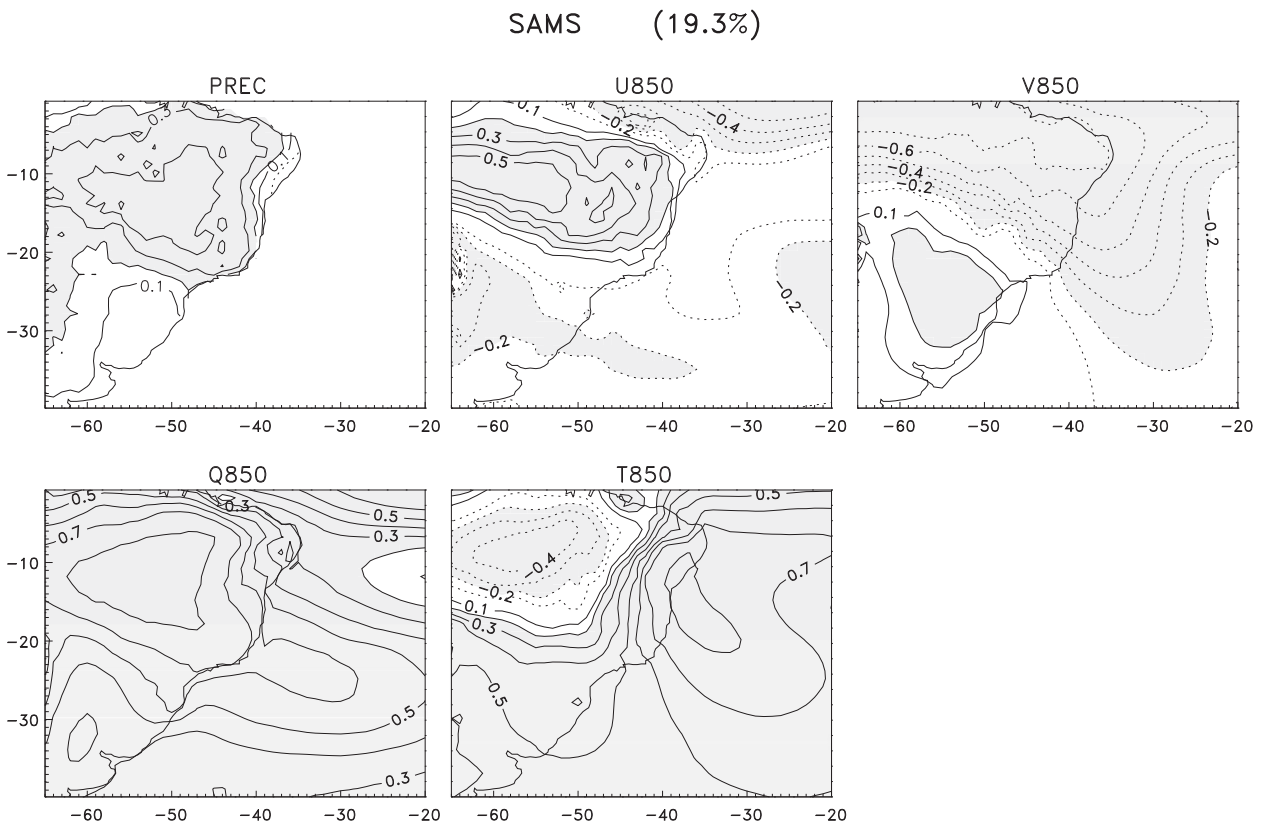

FIG. 2. First spatial pattern (EOF1) from combined EOF analysis of PREC (CPCU), U850, V850, Q850, and T850 (CFSR). EOF is represented as correlations between PC1 and PREC, U850, V850, Q850, and T850 anomalies. Solid (dashed) lines indicate positive (negative) correlations at 0.1 intervals. Shadings indicate correlations greater (less) than 0.2 (−0.2) and significant at the 5% level. Percentage of total variance explained by EOF1 is 20.6%. Period spans 1 Jan 1979–31 Dec 2010.

moisture field (Q850) shows positive anomalies over the core of the monsoon and coincides with negative T850 anomalies due to extensive and persistent cloudiness.

The large-scale features of onset, demise, duration, and amplitude are derived from the time coefficient of the EOF1 [first principal component (PC1)]. Figure 3 shows a 300-day segment of PC1 from 1 September to 30 June 2004–05. The smoothed PC1 is obtained with 15 passes of a 15-day moving average. This smoothing procedure is obtained empirically and used to make the determination of onset, demise, and duration less sensitive to high-frequency variations during the transition phases of the SAMS. The large-scale onset of the SAMS is defined as the date when the smoothed PC1 changes from negative to positive values. This implies that positive precipitation anomalies during that time become dominant over the SAMS domain (Fig. 2). Likewise, the demise date occurs when the smoothed PC1 changes from positive to negative values; duration is the period between onset and demise. The amplitude of the monsoon is defined as the integral of positive unsmoothed PC1 values from onset to demise (Fig. 3). Thus, the amplitude is proportional to cumulative increments of precipitation, moisture, temperature, and atmospheric circulation of the monsoon. Note that intraseasonal variations may occur randomly near the transition phases of SAMS, and break periods are particularly frequent on intraseasonal time scales (e.g., Jones and Carvalho 2002). Thus, this procedure excludes the effect of ''break'' periods in the monsoon near the onset and demise dates (Fig. 3) and makes the index of seasonal amplitudes more robust and less prone to random signals. Last, we point out that the methodology used in this study is different than the one discussed in Bombardi and Carvalho (2009); that study defines local onset and demise dates based on yearly precipitation accumulations (Liebmann and Marengo 2001) and does not consider changes in atmospheric circulation, moisture, and temperature.

Figure 4 shows the summer amplitudes of SAMS during 1979–2010. A prominent feature is the systematic increase in amplitudes especially after the mid-1990s. The statistical significance of the linear trends is estimated by resampling the seasonal amplitudes 10 000 times and fitting linear trends to each batch. The angular

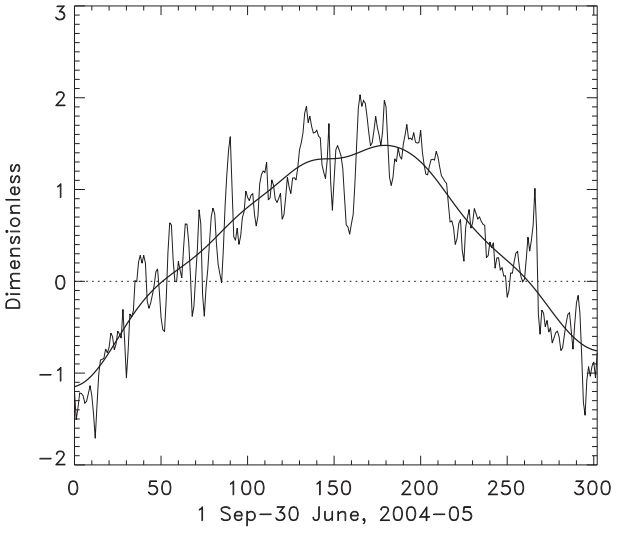

FIG. 3. Example of PC1 (thin solid; dimensionless). Thick solid line indicates smoothed PC1 (15 passes of a 15-day moving average). Period is daily, 1 Sep 2004–30 Jun 2005.

coefficient of the observed linear trend is compared against the sample of 10 000 randomly generated angular coefficients and deemed significant if above the 90th or 95th percentiles. The linear trend is statistically significant at a 5% level.

Figure 5 shows the dates of onset (top), demise (middle), and duration (bottom) of the SAMS and indicates a tendency for early onsets, late demises, and longer durations of the monsoon in South America. All linear trends are statistically significant at the 5% level.

4. Changes in large-scale characteristics of the SAMS: CMIP5 historical experiment

Figure 6 shows the mean daily precipitation during the peak of the monsoon (January–February) obtained from CMIP5 simulations of the historical experiment. The average is performed on a 30-yr period (1976–2005) for comparison with CPC-unified data. A few models are able to simulate the maximum precipitation over the core of the monsoon (cf. Fig. 1), while several models have serious deficiencies: excessive precipitation over northeast Brazil (MPI-ESM-LR), displaced ITCZ (NorESM-M, CanESM2, MRI-CGCM3, and MIROC4h), double ITCZ (GFDL-ESM2M, MPI-ESM-LR, NorESM1-M, IPSL-CM5A-LR, and INM-CM4), and too little precipitation over the eastern Amazon (near the mouth of the Amazon River).

While the intent of this study is not to develop a comparison between CMIP3 and CMIP5, persistent inaccuracies or relative improvements can be seen for some models (cf. with Fig. 2 in Bombardi and Carvalho 2009). The CMIP5 Geophysical Fluid Dynamics Laboratory

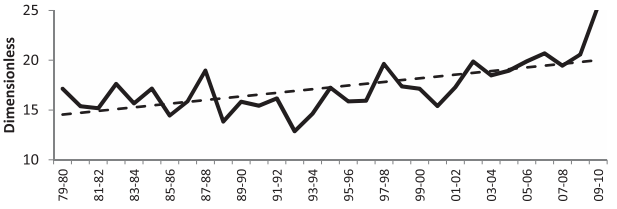

FIG. 4. Seasonal amplitudes (solid line) of the SAMS (dimensionless) determined from PC1 of combined EOF analysis of PREC (CPCU), U850, V850, Q850, and T850 (CFSR; see text for details). Period spans 1 Jan 1979–31 Dec 2010. Dashed line shows linear trend statistically significant at the 5% level.

(GFDL) model represents the maximum precipitation over the SAMS better than its CMIP3 version, although double ITCZ is a persistent feature in that model. Notable improvements in representing the summer season climatology are seen in the CMIP5 versions of MPI, MRI (cf. also with Blázquez and Nuñez 2013), and MIROC. No improvements are seen in the CMIP5 CSIRO model as far as the representation of the SAMS is concerned.

The same methodology described in the previous section to obtain the large-scale characteristics of the SAMS (i.e., amplitude, onsets, demises, and durations) is applied to the 10 CMIP5 model simulations from the historical experiment: combined EOF of PREC, U850,

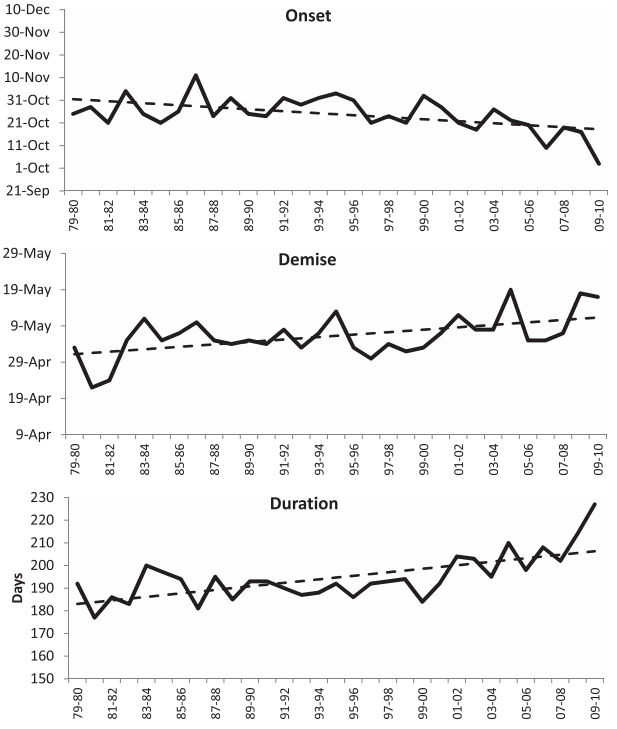

FIG. 5. (top) Onset, (middle) demise, and (bottom) duration of the SAMS (see text for details). Period spans 1 Jan 1979–31 Dec 2010. Dashed lines show linear trends statistically significant at the 5% level.

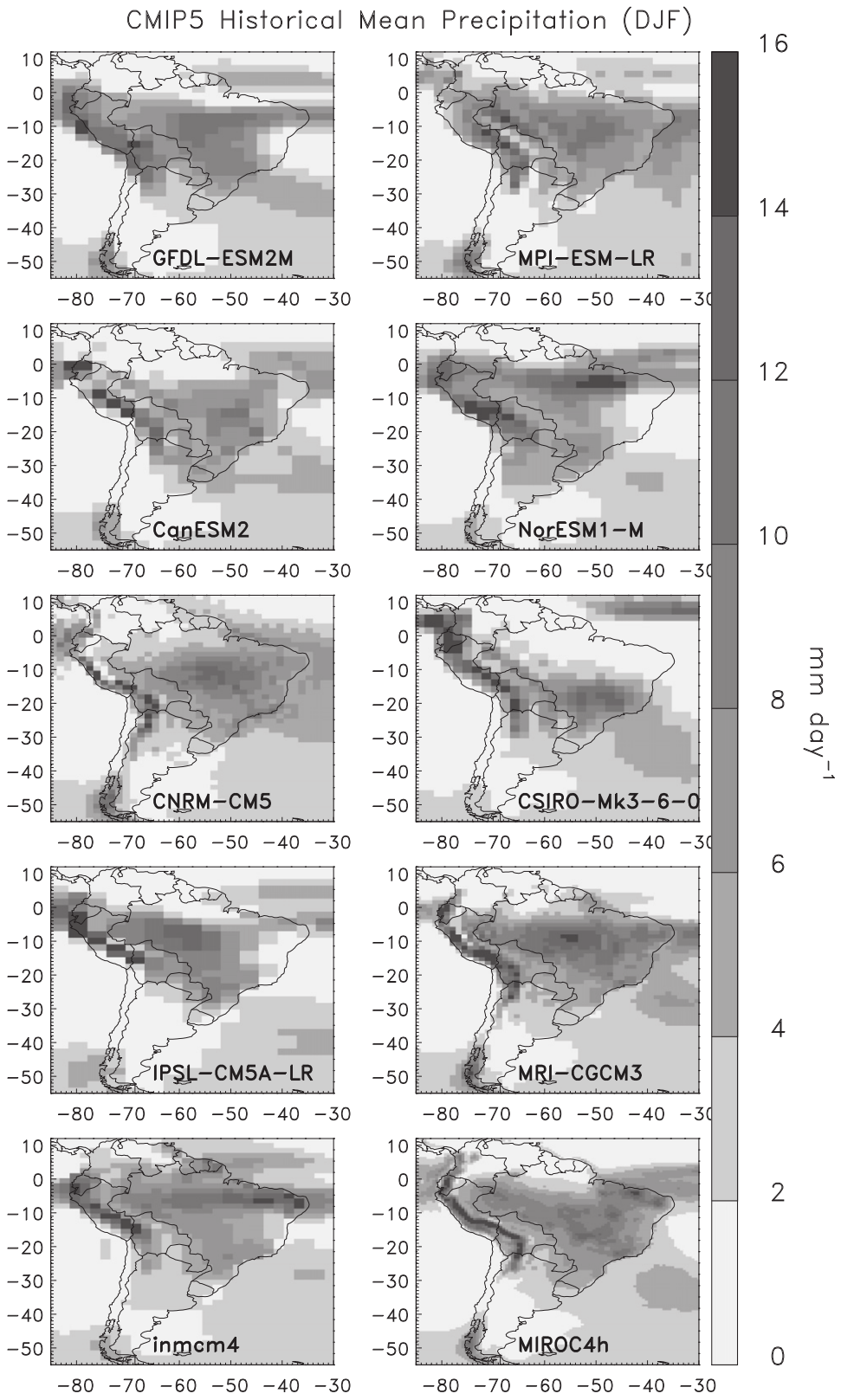

FIG. 6. Mean precipitation (mm day^{-1}) during January–February derived from CMIP5 model simulations for the historical experiment (30-yr average; 1976–2005).

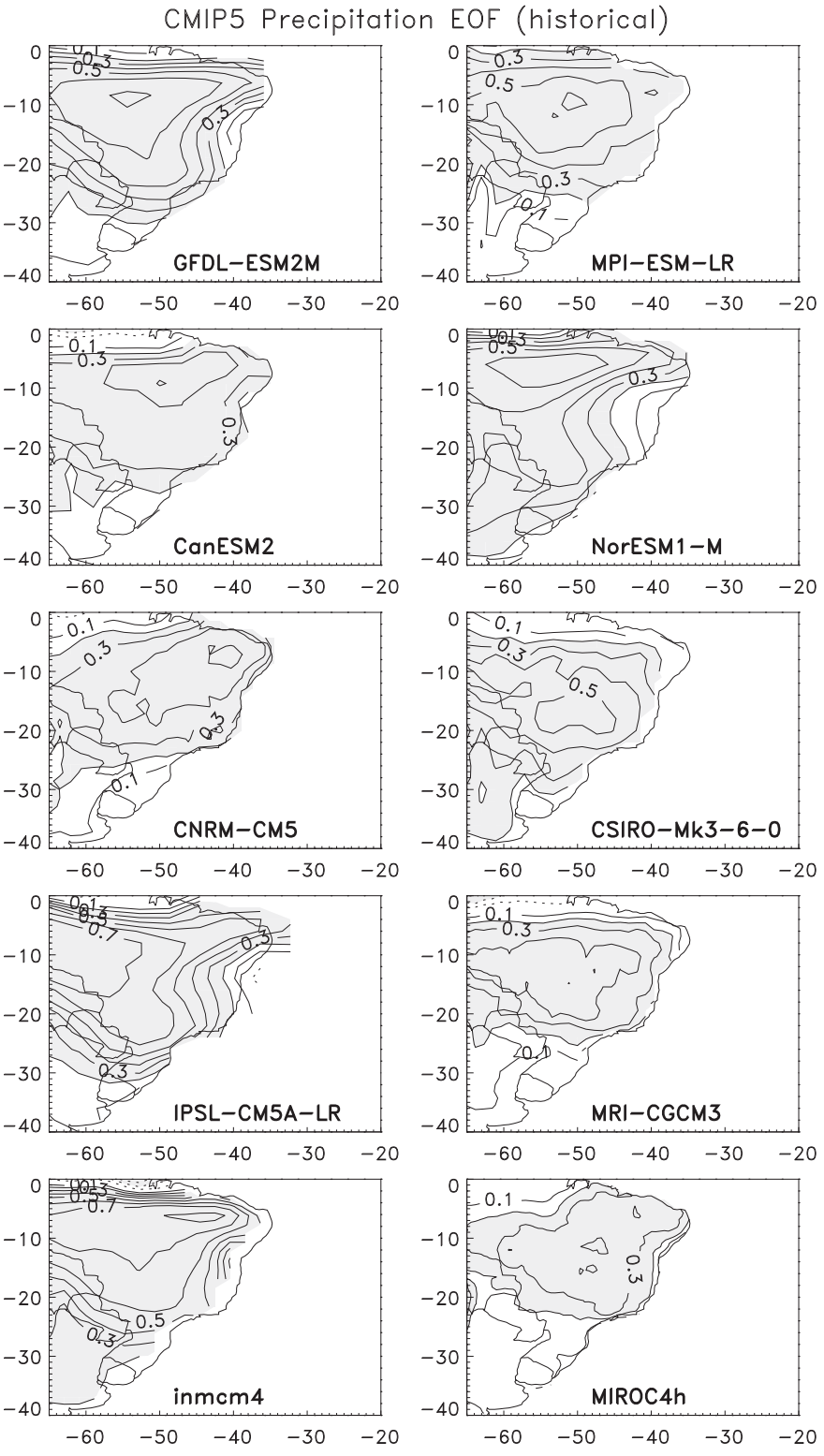

FIG. 7. First EOF of precipitation obtained from combined EOF of PREC, U850, V850, Q850, and T850 anomalies. EOF is represented as correlation between PC1 and PREC anomalies. Solid (dashed) lines indicate positive (negative) correlations (0.1 intervals). Shadings indicate correlations greater (less) than 0.2 (−0.2) and significant at the 5% level. Period spans CMIP5 simulations of historical experiment.

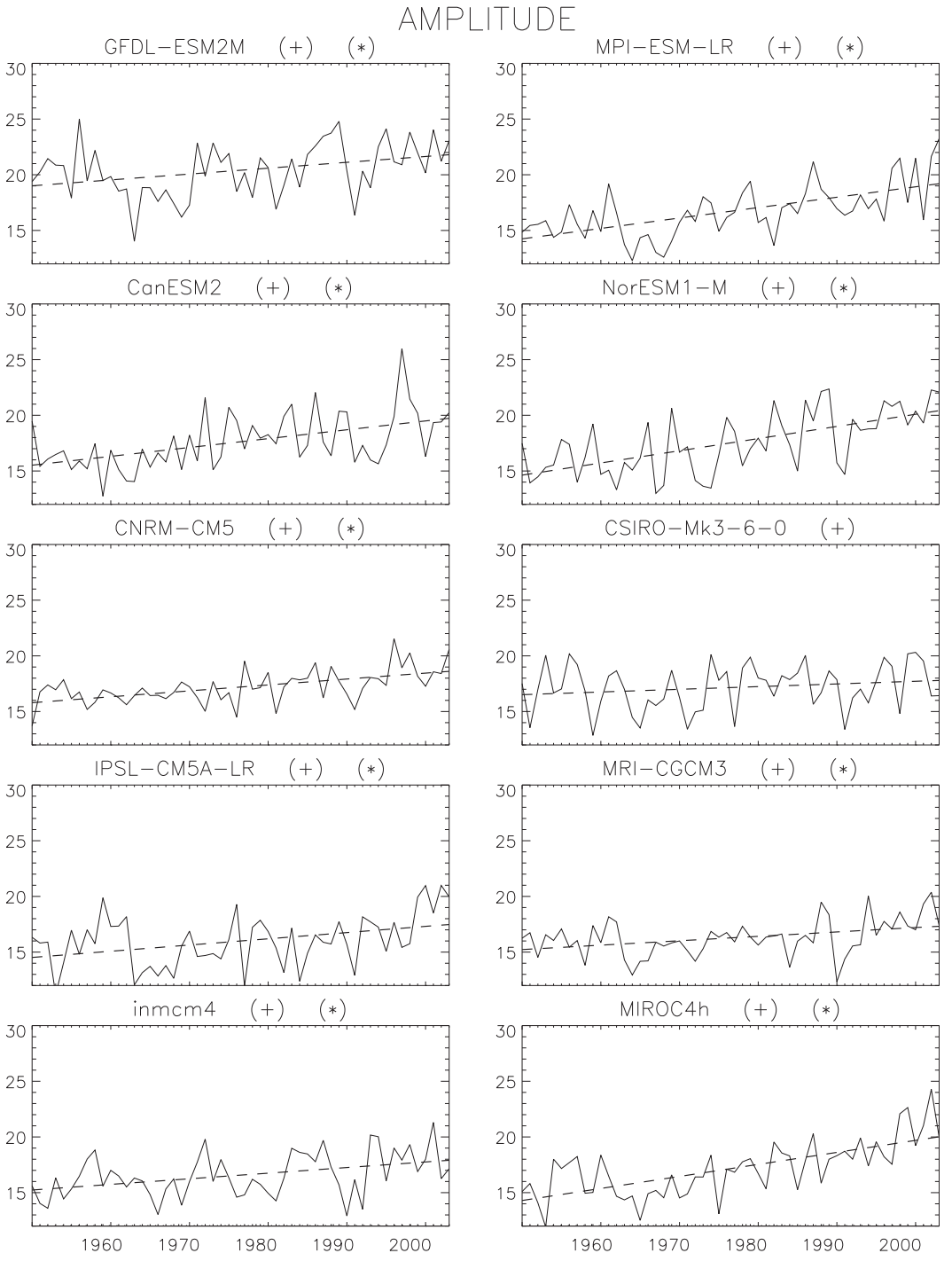

FIG. 8. Seasonal amplitudes of the SAMS (dimensionless) obtained from CMIP5 model simulations for the historical experiment. Dashed lines show linear fit; "+" and "*" next to model name indicate that linear trend is statistically significant at 10% and 5%, respectively. Periods spans 1 Jan 1951–31 Dec 2005.

V850, Q850, and T850. In the interest of space, we discuss the first EOF. The amount of total variance expressed by EOF1 for each model is 21.5% (CanESM2), 25.6% (CNRM-CM5), 22.3% (CSIRO-Mk3.6.0), 26.1% (GFDL-ESM2M), 23.4% (INM-CM4), 25.6% (IPSL-CM5A-LR), 17.6% (MIROC4h), 27.5% (MPI-ESM-LR), 24.2% (MRI-CGCM3), and 27.0% (NorESM1-M). Figure 7 shows the precipitation variability associated with EOF1 expressed as correlations between PC1 and PREC anomalies. Some models (e.g., MPI-ESM-LR, MRI-CGCM3,

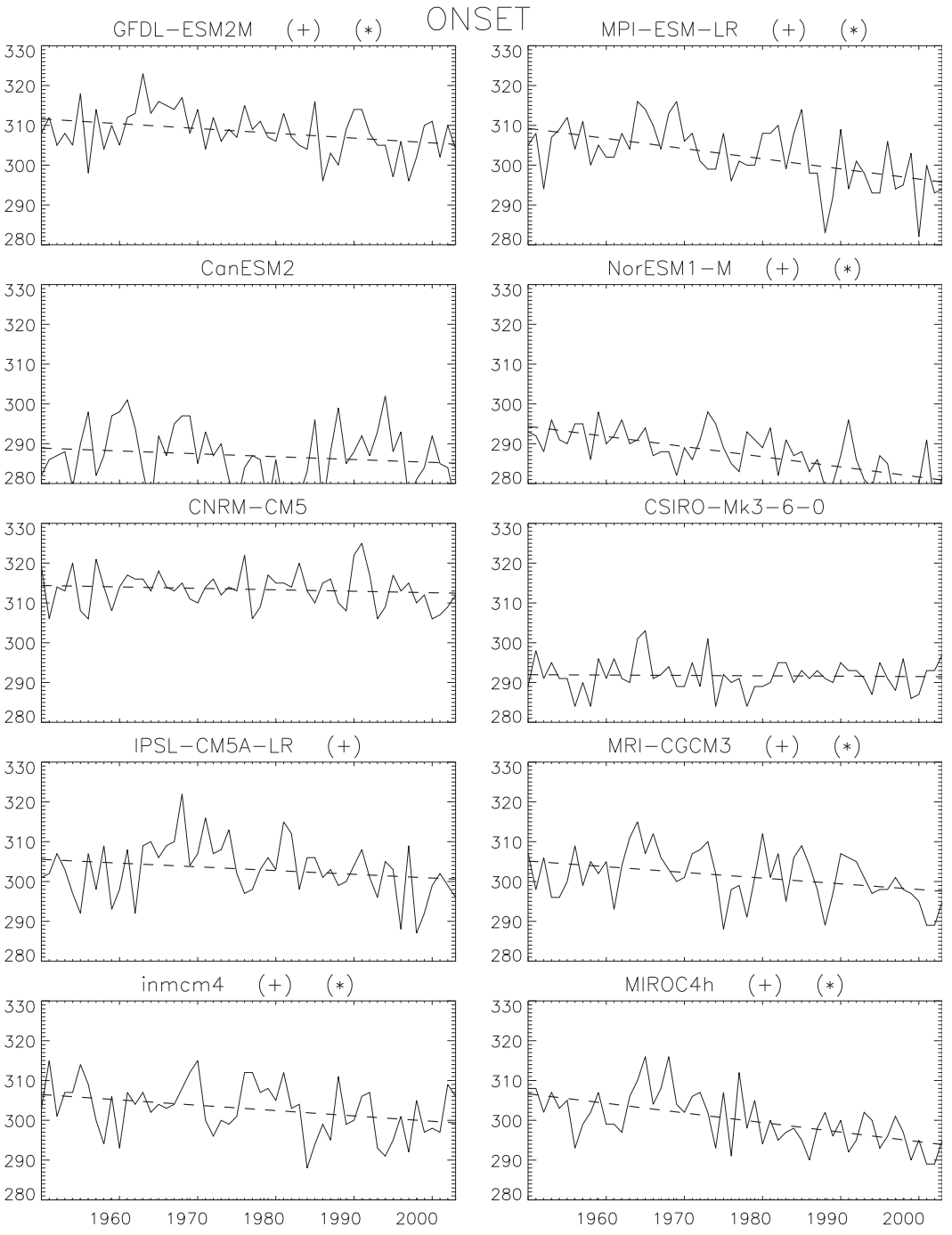

FIG. 9. As in Fig. 8, but for onset dates of the SAMS obtained from CMIP5 model simulations for the historical experiment. Vertical axis shows day of the year (1 = 1 Jan, 360 = 31 Dec). Period spans 1 Jan 1951–31 Dec 2005.

and MIROC4h) are quite realistic in capturing the observed maximum precipitation variability over the Amazon and central Brazil (cf. with Fig. 2). Other models show the maximum precipitation variability displaced in a zonally elongated band south of the equator (e.g., CanESM2, NorESM1-M, INM-CM4), to the west (IPSL-CM5A-LR), or east (e.g., CNRM-CM5, INM-CM4). The spatial variability of precipitation in the GFDL-ESM3M is comparable (e.g., correlation above 0.2) to the observations, although the maximum is too far north relative to the CPCU data. Although the precipitation spatial variability in the CSIRO-Mk3.6.0 model

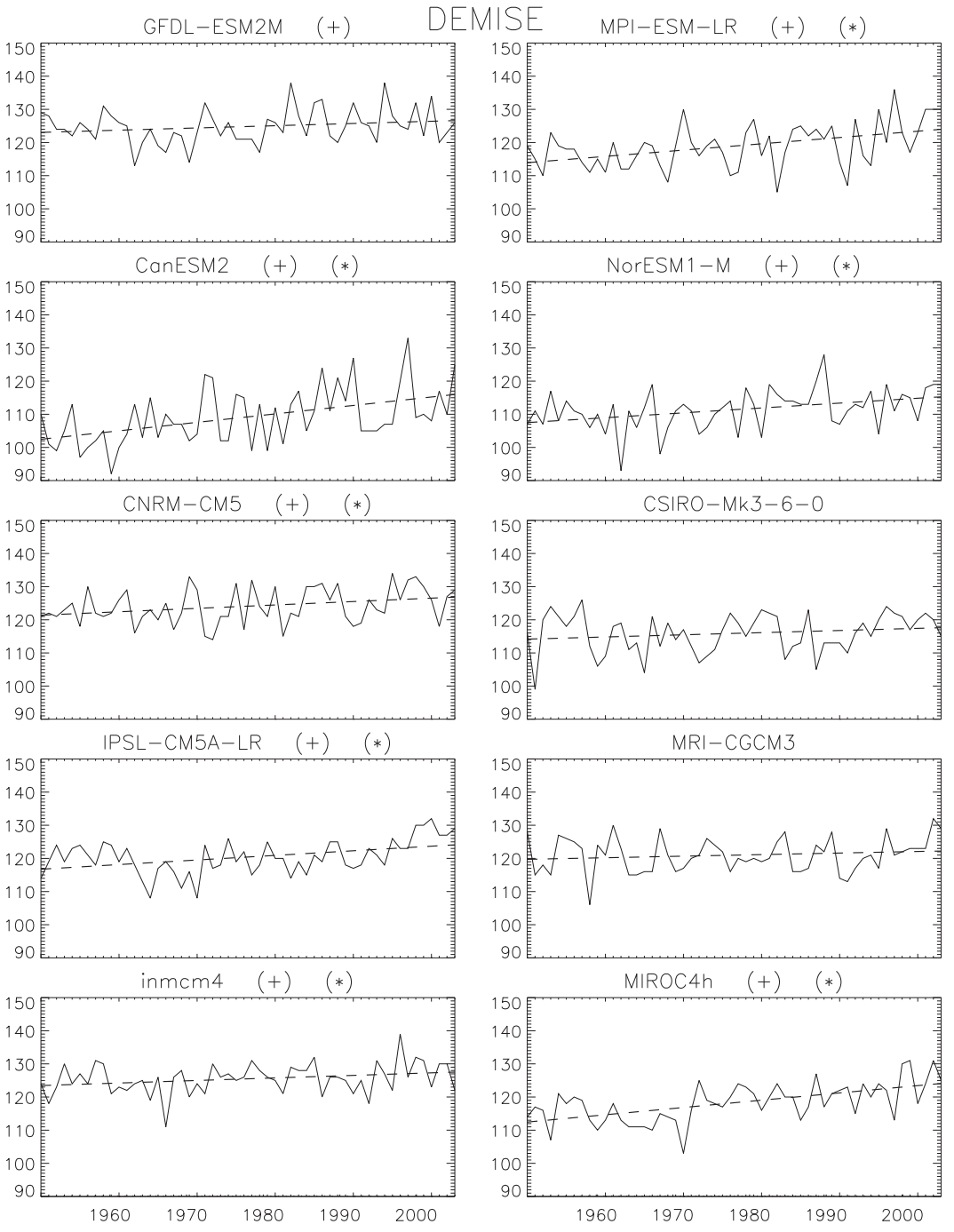

FIG. 10. As in Fig. 9, but for demise dates of the SAMS obtained from CMIP5 model simulations for the historical experiment. Vertical axis shows day of the year (1 = 1 Jan, 360 = 31 Dec). Period spans 1 Jan 1951–31 Dec 2005.

shows the maximum over central Brazil (Fig. 7), the model clearly has problems in representing the mean precipitation (cf. Figs. 2 and 6). The variability of U850, V850, Q850, and T850 associated with EOF1 for all 10 models agrees fairly well with the reanalysis (Fig. 2) and is not shown.

Figure 8 shows the amplitude of the SAMS derived from CMIP5 model simulations of the historical experiment. Linear trends are shown by dashed lines. The statistical significance of the linear trends is estimated by resampling the seasonal amplitudes 10 000 times and fitting linear trends to each batch. The angular

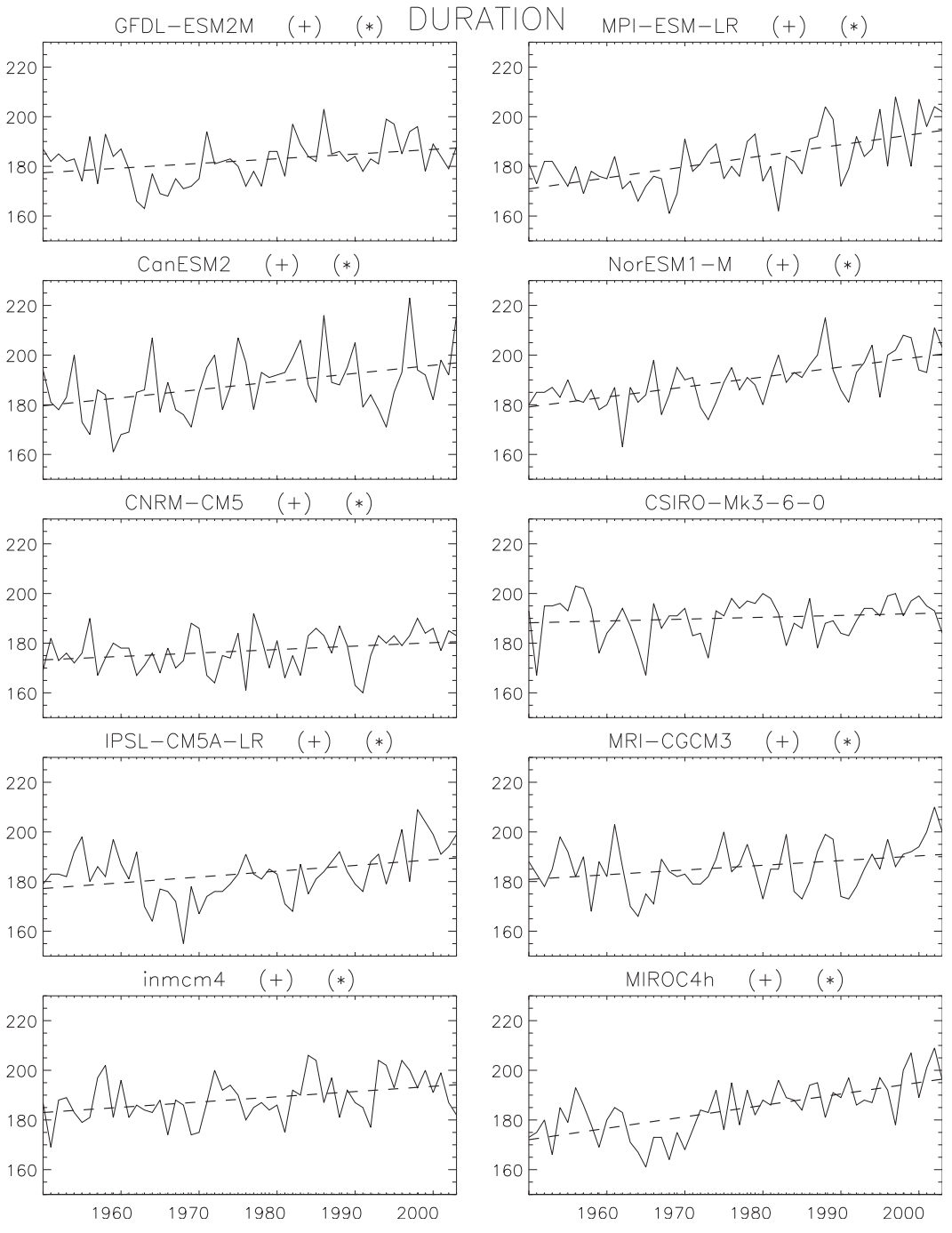

FIG. 11. As in Fig. 10, but for duration of the SAMS obtained from CMIP5 model simulations for the historical experiment. Period spans 1 Jan 1951–31 Dec 2005.

coefficient of the linear trend obtained from the historical simulation (Fig. 8) is compared against the sample of 10 000 randomly generated angular coefficients and deemed significant if above the 90th or 95th percentiles. Nine out of the 10 CMIP5 simulations of the historical experiment show positive and statistically significant (5% level) trends in the amplitude of the SAMS (Fig. 8). The linear trend obtained with the CSIRO-Mk3.6.0 model is only significant at the 10% level. The rates of increase in the amplitude of the SAMS vary among the models and are summarized in section 5.

CMIP simulations of the historical experiment also indicate changes in the onset dates of the monsoon (Fig. 9). All 10 models show negative linear trends indicating that the onset of the SAMS in recent years occurs earlier than in previous years, although the magnitudes of the linear trends vary among the models. Statistical significance is estimated as described above. Six out of the 10 models show statistically significant trends at the 5% level. It is also worth noting that some models (IPSL-CM5A-LR, MRI-CGCM3, INM-CM4, and MIROC4h) show average onset dates very close to the observed average values determined by CPCU and CFSR data (day 299 or 26 October). In contrast, other models exhibit onset dates much earlier (CanESM2 and NorESM1-M), much later (CNRM-CM5), or with much less interannual variations (CSIRO-Mk3.6.0) than observations.

On the other hand, all 10 CMIP5 model simulations of the historical experiment show positive increases in the dates of demise of the SAMS (Fig. 10), although the magnitudes vary among the models. Trends are statistically significant (5% level) in seven model simulations. Several models show demise dates consistent with observed average values determined by reanalyses (day 127 or 7 April). Exceptions are NorESM1-M and CSIRO-Mk3.6.0 models with demise dates much earlier than observations. Figure 11 shows changes in the duration of the SAMS estimated by CMIP5 model simulations of the historical experiment. Nine out of 10 models show positive and statistically significant (5% level) trends in the duration of the SAMS.

Last, it is relevant to note an important aspect about the trends in the characteristics of the SAMS derived from CPCU/CFSR and CMIP5 model simulations. The amplitude, onset, demise, and duration of the monsoon are determined from combined EOF of PREC, U850, V850, Q850, and T850. Additional tests were performed by computing EOF of each variable separately. The results indicate that all variables have significant trends (not shown).

5. Projections of large-scale changes in the SAMS: CMIP5 rcp8.5 scenario

Future changes in the SAMS during 2006–2100 are evaluated with CMIP5 model simulations of the rcp8.5 scenario. The large-scale characteristics of amplitude, onset, demise, and duration of the SAMS are determined from combined EOF of PREC, U850, V850, Q850, and T850 from six CMIP5 model simulations (Table 1). Each CMIP5 simulation of the rcp8.5 scenario shows substantial increases in amplitude, early onsets, late demises, and increases in the duration of the SAMS (not shown).

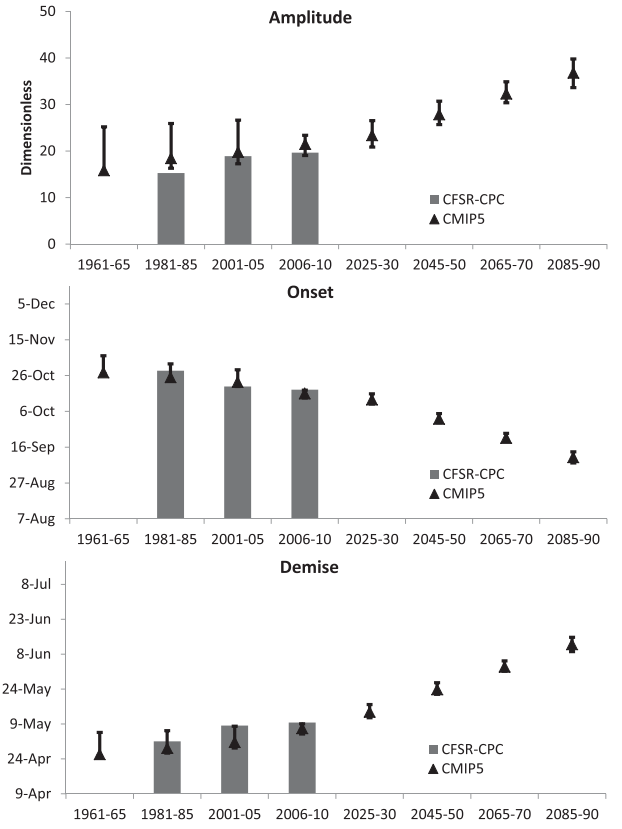

FIG. 12. Decadal changes in the SAMS (top) amplitude, (middle) onset, and (bottom) demise dates. Gray bars show changes obtained from CPCU/CFSR. Triangles indicate ensemble means of CMIP5 simulations for the historical (1961–2005) and rcp8.5 (2006–90) experiments. Tips of the vertical lines show minimum and maximum values. Changes are estimated in 5-yr periods (horizontal axis). Number of CMIP5 models used were 10 (historical) and 6 (rcp8.5).

To summarize the results, Fig. 12 (top) shows 5-yr means of the seasonal amplitudes of the SAMS. These values are calculated from the linear fit of seasonal amplitudes (e.g., Fig. 4 for CPCU/CFSR). The focus is on decadal changes in amplitudes of the SAMS and the calculation is performed for CPCU/CFSR (bars; 1981–2010) and CMIP5 model simulations of the historical and rcp8.5 experiments. CMIP5 ensemble means are indicated by triangles, whereas the tips of the vertical bars show minimum and maximum values. As discussed previously, CPCU/CFSR indicates increases in mean amplitudes during 1981–2010. It is worth noting the difference in mean value between CPCU/CFSR and CMIP5 ensemble mean during 1981–2010. This is likely associated with the fact that CMIP5 historical simulations are initialized from arbitrary points in time (Taylor et al. 2012) and do not predict the same observed interannual changes in the monsoon. It is also interesting to see that

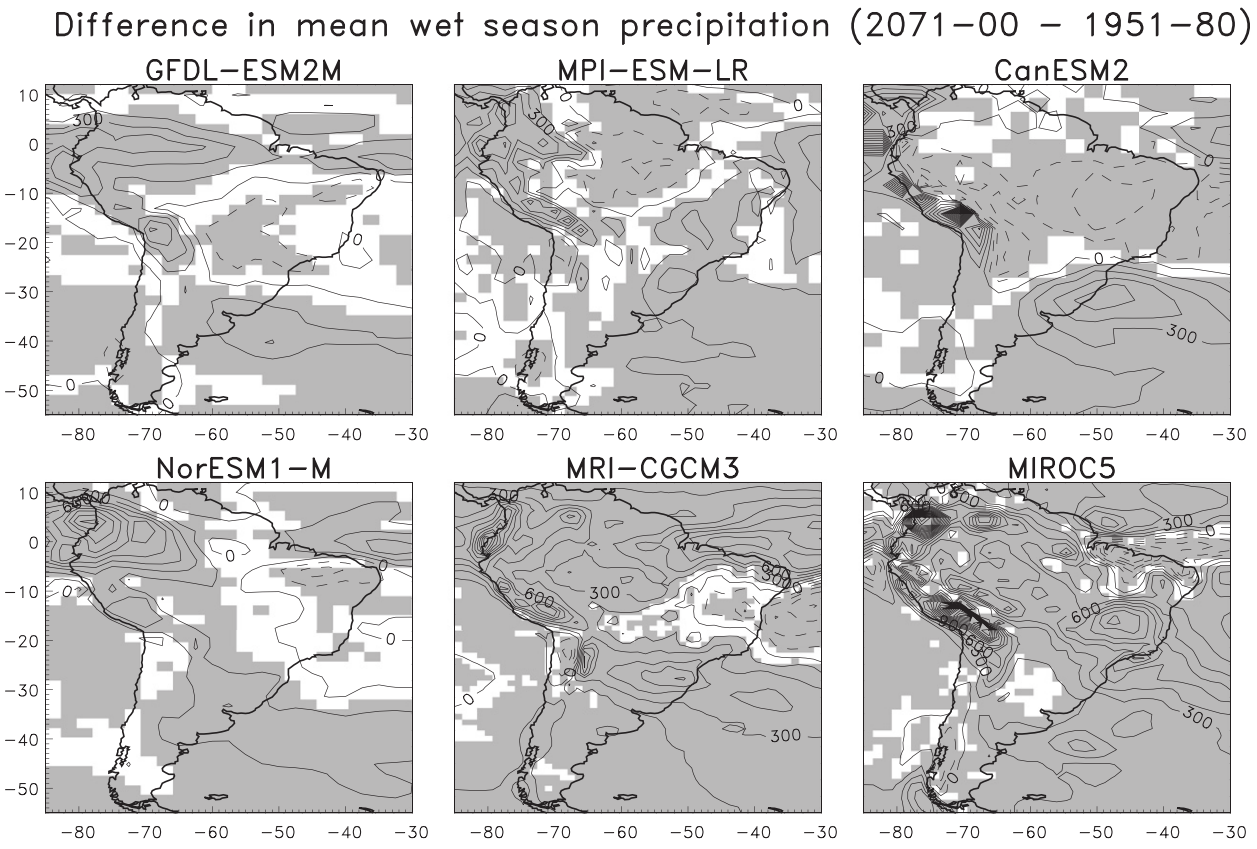

FIG. 13. Difference between mean total wet-season precipitation during 2071–2100 and 1951–80. Wet-season precipitation is computed as the total from onset to demise dates of SAMS and averaged during 2071–2100 and 1951–80. Solid (dashed) lines indicate positive (negative) values (150 mm day^{-1} interval). Shaded regions are statistically significant at the 5% level. Note, MIROC difference is computed between MIROC5 and MIROC4h.

the spread among the models is skewed to high amplitudes and larger during 1961–2005 than in subsequent years. Additionally, CMIP5 simulations of the rcp8.5 scenario coherently indicate positive trends in the amplitude of the SAMS during 2025–90. The simulations for this scenario project mean amplitude of ~28 by 2045–50 representing a 30% increase to the mean value simulated by the models during 2006–10.

Similarly, Fig. 12 (middle) shows 5-yr means of onset dates obtained from CPCU/CFSR and CMIP5 model simulations of the historical and rcp8.5 experiments. CMIP5 model simulations systematically show early onsets of the monsoon during 1961–2010 and continue in the rcp8.5 scenario (2025–90). It is particularly concerning that the rcp8.5 scenario projects an ensemble mean decrease of 14 day in the onset of the SAMS by 2045–50 relative to the mean value simulated by the models during 2006–10.

The temporal evolution of 5-yr means of demise dates of the SAMS during 1961–2010 (Fig. 12, bottom) is coherent between CPCU/CFSR and CMIP5 simulations of the historical experiment. The ensemble mean projected values from the rcp8.5 experiment suggest a 17-day increase in the demise date of the SAMS by 2045–50 relative to the mean value simulated by the models during 2006–10.

The results of model simulations indicate considerable changes in the large-scale characteristics of the SAMS during 1961–2010. The rcp8.5 high-emission scenario projects even more substantial changes for the twenty-first century. To investigate potential changes in precipitation associated with the SAMS, we used the CMIP5 historical simulations to compute the total precipitation from onset to demise for each wet season during 1951–80. Likewise the total precipitation from onset to demise during 2071–2100 was calculated from CMIP5 rcp8.5 simulations. Figure 13 shows the difference in mean total precipitation between 2071 and 2100 and 1951 and 1980. The GFDL-ESM2M projects less total wet-season precipitation over central-eastern Brazil, but increased precipitation over northwestern South America and farther south over southern Brazil, Uruguay, and northern

Argentina. MPI-ESM-LR projects increases in precipitation over much of eastern and northwestern South America and decreased precipitation over the northern Amazon. The CanESM2 also projects increased precipitation over subtropical latitudes and the central Andes, but decreased precipitation over most of tropical South America. In agreement with GFDL-ESM2M, the NorESM1-M projects increases in precipitation from Argentina and Uruguay toward the northwestern South America. MRI-CGCM3 projects increases in monsoon season precipitation over most of South America and less precipitation over northeast Brazil. In contrast, MIROC5 projects increases in precipitation over most of South America and high increases in orographic precipitation over the Andes. The lack of spatial agreement in the projections is evident among the models.

A thorough comparison with CMIP3 model projections discussed in Bombardi and Carvalho (2009) is not possible, given the differences in models analyzed and methodologies. Nevertheless, the CMIP3 GFDL model projects decreases in total precipitation over central-eastern Brazil and increases in precipitation over southern Brazil (see their Fig. 13). As discussed previously, however, the CMIP5 GFDL model represents the SAMS better than the CMIP3 version. Projections in total wet-season precipitation are consistent between both versions of the MPI model, although the CMIP5 MPI model captures the mean SAMS precipitation considerably better than the CMIP3 version.

Low-level moisture divergence can be used to gain further insight into changes in the precipitation patterns over the SAMS. Daily moisture divergence (850 hPa) from CFSR reanalysis was computed for the period from 1 January 1979 to 31 December 2010. To focus on changes in precipitation over the monsoon, the integral of negative moisture divergence (i.e., moisture convergence) was computed from onset to demise for each wet season (1979–2010) and each grid point in the analysis domain. Next, the linear trend was computed and statistical significance (5% level) was assessed by resampling as explained before. Negative trends (Fig. 14) indicating increased moisture convergence are observed over large areas over the northern Amazon, parts of the ITCZ, east of the tropical Andes, and portions of eastern Brazil. Interestingly, the region of increased moisture convergence trend over parts of southern Brazil coincides with the positive trend in precipitation reported by Liebmann et al. (2004b). In addition, regions of positive trends are noted over parts of central and northern Brazil indicating weakening in low-level moisture convergence.

Similar calculations were performed for the CMIP5 historical simulations (1951–2005) to investigate the extent to which models agree or disagree on the trends in low-level moisture convergence (Fig. 15). While some resemblance is noted among some models (GFDL-ESM2M, MPI-ESM-LR, CanESM2, NorESM1-M, IPSL-CM5A-LR, and INM-CM4) in simulating increased moisture convergence over parts of northern South America and parts of northern Argentina and southern Brazil, it is clear that significant disagreements are noted among the models as far as trends in low-level moisture convergence are concerned. Trends in low-level moisture convergence obtained from CMIP5 rcp8.5 simulations are shown in Fig. 16. While models project increases in moisture convergence over most of South America, large differences in regional changes and magnitudes are noted among the models.

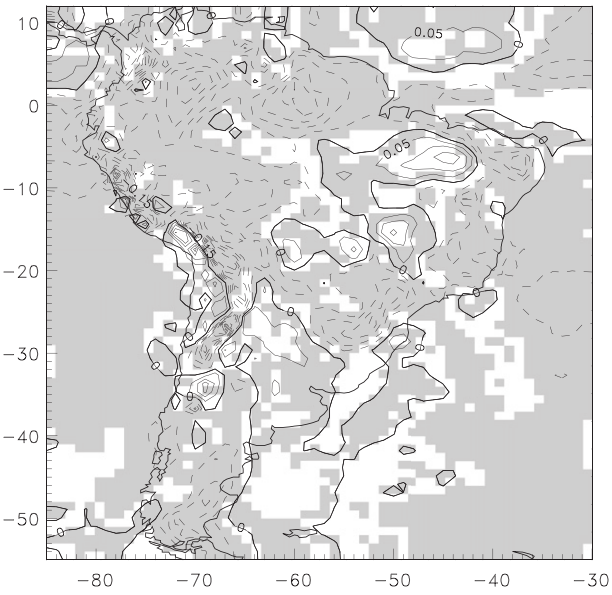

FIG. 14. Linear trend in negative low-level moisture divergence (850 hPa; units $\times 10^{-6}\,s^{-1}$) from CFSR reanalysis. Field is integrated from each onset to demise dates of the SAMS during 1979–2010. Solid (dashed) contours indicate positive (negative) trends at 0.05 intervals. Shading indicates trends statistically significant at the 5% level.

6. Summary and conclusions

This study documents changes in the large-scale characteristics of the SAMS using CPCU precipitation, CFSR reanalysis, and CMIP5 model simulations of the historical and rcp8.5 experiments. The large-scale features of amplitude, onset, demise, and duration of the SAMS are determined from combined EOF analysis of PREC, U850, V850, Q850, and T850. The CPCU/CFSR analysis shows statistically significant trends and indicates increased seasonal amplitudes, early onsets, late demises, and longer durations in the decades from 1979–2010.

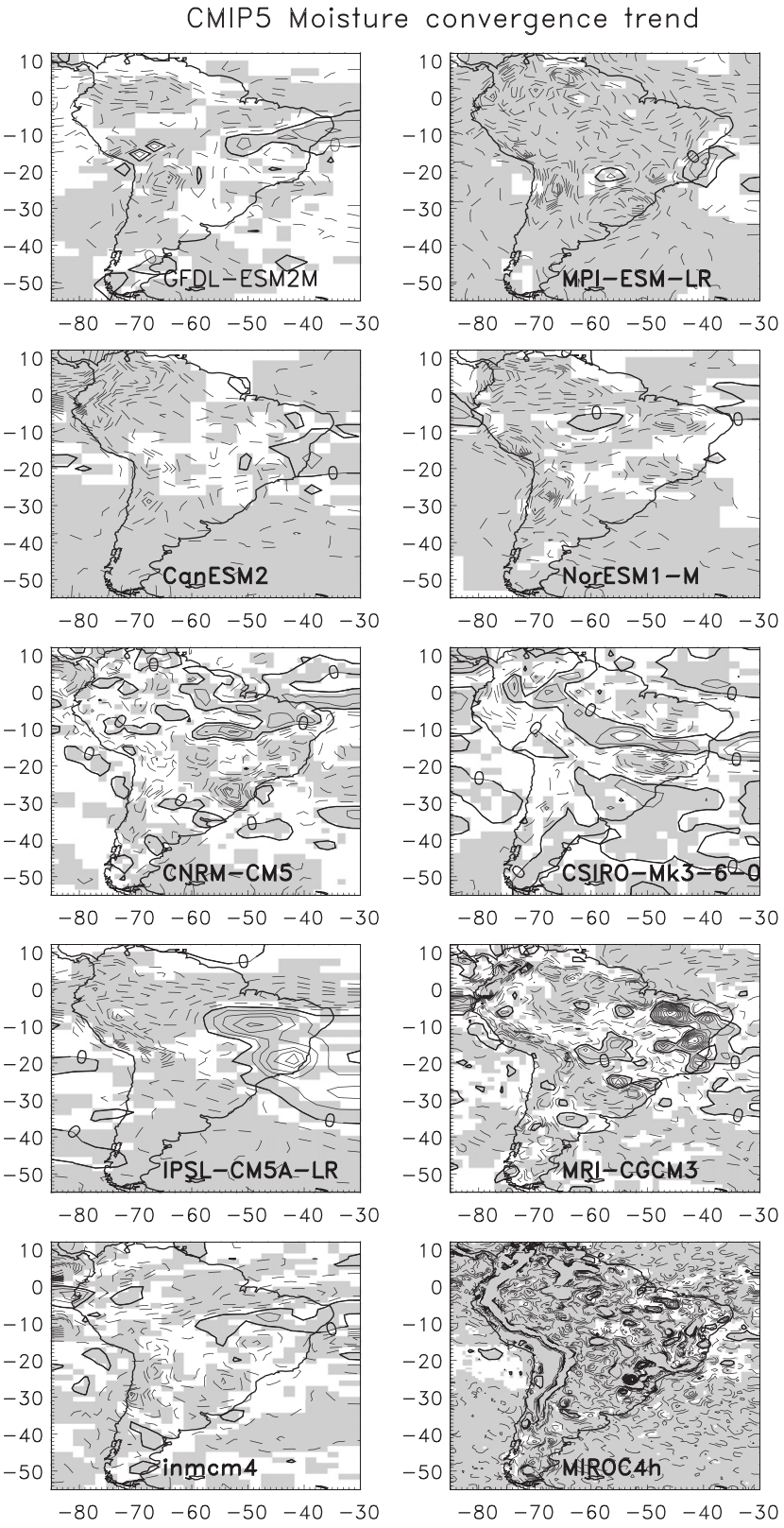

FIG. 15. As in Fig. 14, but for linear trends derived from CMIP5 historical model simulations.

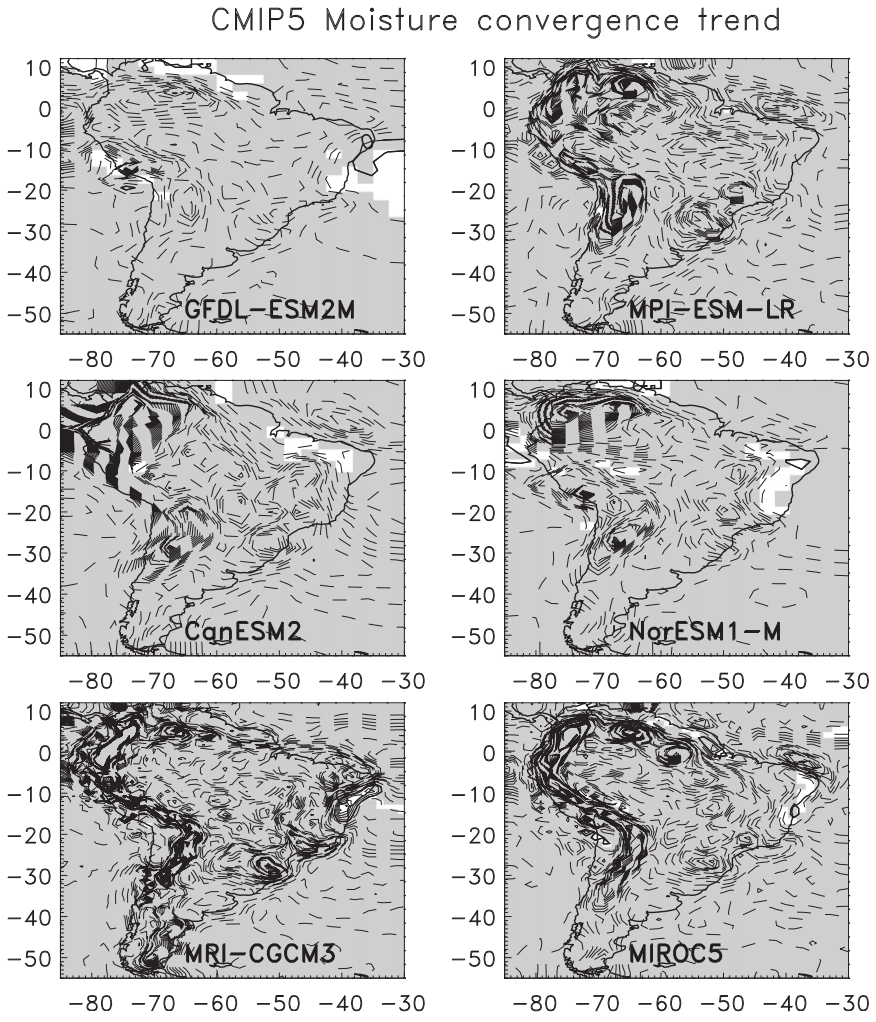

FIG. 16. As in Fig. 14, but for linear trends derived from CMIP5 rcp8.5 model simulations.

Some of the 10 CMIP5 model simulations of the historic experiment analyzed in this study show relatively good skill in representing U850, V850, Q850, and T850 and to some degree the mean and variance of precipitation associated with the SAMS. This study demonstrates that CMIP5 model simulations of the historical experiment coherently show positive increases in the amplitude, early onset, late demise, and duration of the SAMS during 1951–2005.

Future changes in the SAMS are analyzed with six CMIP5 model simulations of the rcp8.5 high-emission scenario. Most of the simulations show significant increases in seasonal amplitudes, early onsets, late demises, and durations of the SAMS. The simulations for this scenario project a 30% increase in the amplitude from the current level by 2045–50. In addition, the rcp8.5 scenario projects an ensemble mean decrease of 14 days in the onset and 17-day increase in the demise date of the SAMS by 2045–50.

It is relevant to highlight some additional conclusions. The methodology employed in this study characterizes the large-scale properties of amplitude, onset, demise, and duration of the SAMS. CMIP5 model simulations show signals of climate change in South America. While the observational data show trends, the period used is too short for final conclusions concerning climate change. Furthermore, despite differences in methodologies and models analyzed, a comparison with a previously published paper (Bombardi and Carvalho 2009) indicates that some CMIP5 models have significantly improved their representation of the SAMS, while other models exhibit persistent deficiencies.

How precipitation during the SAMS will change in the coming decades is still an open question. Using CMIP3 simulations, Seth et al. (2010, 2011) argue for reduced precipitation during onset months over the central monsoon region and increases at the end of the monsoon life cycle. However, since specific definitions of onset and

demise dates are not provided in that study, we are not able to draw further comparisons with the results presented here. The results in this study indicate lack of spatial agreement in the CMIP5 model projections of changes in total wet-season precipitation over South America. The most consistent CMIP5 projections analyzed here are the increase in the total monsoon precipitation over southern Brazil, Uruguay, and northern Argentina.

Acknowledgments. C. Jones and L. M. V. Carvalho thank the financial support of the National Science Foundation Rapid Program (AGS-1126804) and NOAA Climate Program Office (NA10OAR4310170). This research was conducted under the CGIAR Research Program on Climate Change, Agriculture and Food Security (CCAFS), and benefited from a subcontract with the International Potato Center in Lima, Peru (SB120184). CFSR reanalysis for this study are from the Research Data Archive (RDA) which is maintained by the Computational and Information Systems Laboratory (CISL) at the National Center for Atmospheric Research (NCAR). NCAR is sponsored by the National Science Foundation (NSF). We acknowledge the World Climate Research Programme Working Group on Coupled Modeling, which is responsible for CMIP, and we thank the climate modeling groups (listed in Table 1 of this paper) for producing and making available their model output. For CMIP, the U.S. Department of Energy's Program for Climate Model Diagnosis and Intercomparison provides coordinating support and led development of software infrastructure in partnership with the Global Organization for Earth System Science Portals. Comments and suggestions from anonymous reviewers are greatly appreciated.

REFERENCES

Berbery, E. H., and E. A. Collini, 2000: Springtime precipitation and water vapor flux over southeastern South America. *Mon. Wea. Rev.,* **128,** 1328–1346.

——, and V. R. Barros, 2002: The hydrologic cycle of the La Plata basin in South America. *J. Hydrometeor.,* **3,** 630–645.

Blázquez, J., and M. N. Nuñez, 2013: Performance of a high resolution global model over southern South America. *Int. J. Climatol.,* **33,** 904–919.

Bombardi, R. J., and L. M. V. Carvalho, 2009: IPCC global coupled climate model simulations of the South America monsoon system. *Climate Dyn.,* **33,** 893–916.

Bookhagen, B., and M. R. Strecker, 2008: Orographic barriers, high-resolution TRMM rainfall, and relief variations along the eastern Andes. *Geophys. Res. Lett.,* **35,** L06403, doi:10.1029/2007GL032011.

——, and D. W. Burbank, 2010: Towards a complete Himalayan hydrologic budget: The spatiotemporal distribution of snowmelt and rainfall and their impact on river discharge. *J. Geophys. Res.,* **115,** F03019, doi:10.1029/2009JF001426.

Carvalho, L. M. V., C. Jones, and B. Liebmann, 2002a: Extreme precipitation events in southeastern South America and large-scale convective patterns in the South Atlantic convergence zone. *J. Climate,* **15,** 2377–2394.

——, ——, and M. A. F. Silva Dias, 2002b: Intraseasonal large-scale circulations and mesoscale convective activity in tropical South America during the TRMM-LBA campaign. *J. Geophys. Res.,* **107** (D20), doi:10.1029/2001JD000745.

——, ——, and B. Liebmann, 2004: The South Atlantic convergence zone: Intensity, form, persistence, and relationships with intraseasonal to interannual activity and extreme rainfall. *J. Climate,* **17,** 88–108.

——, ——, A. E. Silva, B. Liebmann, and P. L. S. Dias, 2011a: The South American monsoon system and the 1970s climate transition. *Int. J. Climatol.,* **31,** 1248–1256, doi:10.1002/joc.2147.

——, A. E. Silva, C. Jones, B. Liebmann, and H. Rocha, 2011b: Moisture transport and intraseasonal variability in the South America monsoon system. *Climate Dyn.,* **36,** 1865–1880, doi:10.1007/s00382-010-0806-2.

Chen, M. Y., W. Shi, P. P. Xie, V. B. S. Silva, V. E. Kousky, R. W. Higgins, and J. E. Janowiak, 2008: Assessing objective techniques for gauge-based analyses of global daily precipitation. *J. Geophys. Res.,* **113,** D04110, doi:10.1029/2007JD009132.

Durieux, L., L. A. T. Machado, and H. Laurent, 2003: The impact of deforestation on cloud cover over the Amazon arc of deforestation. *Remote Sens. Environ.,* **86,** 132–140.

Field, C. B., and Coauthors, Eds., 2012: *Managing the Risks of Extreme Events and Disasters to Advance Climate Change Adaptation.* Cambridge University Press, 582 pp.

Gan, M. A., V. B. Rao, and M. C. L. Moscati, 2006: South American monsoon indices. *Atmos. Sci. Lett.,* **6,** 219–223.

Gandu, A. W., and P. L. Silva Dias, 1998: Impact of tropical heat sources on the South American tropospheric upper circulation and subsidence. *J. Geophys. Res.,* **103,** 6001–6015.

Grimm, A. M., 2003: The El Niño impact on the summer monsoon in Brazil: Regional processes versus remote influences. *J. Climate,* **16,** 263–280.

——, 2004: How do La Niña events disturb the summer monsoon system in Brazil? *Climate Dyn.,* **22,** 123–138.

——, 2011: Interannual climate variability in South America: Impacts on seasonal precipitation, extreme events, and possible effects of climate change. *Stochastic Environ. Res. Risk Assess.,* **25,** 537–554.

——, and M. T. Zilli, 2009: Interannual variability and seasonal evolution of summer monsoon rainfall in South America. *J. Climate,* **22,** 2257–2275.

——, C. S. Vera, and C. R. Mechoso, 2005: The South American monsoon system. WMO/TD 1266 (TMRP Rep. 70), 219–238.

Hartmann, D. L., and E. E. Recker, 1986: Diurnal-variation of outgoing longwave radiation in the tropics. *J. Climate Appl. Meteor.,* **25,** 800–812.

Higgins, R. W., W. Shi, E. Yarosh, and R. Joyce, 2000: Improved United States precipitation quality control system and analysis. *NCEP/Climate Prediction Center ATLAS 7,* National Oceanic and Atmospheric Administration, 40 pp.

——, V. E. Kousky, V. B. S. Silva, E. Becker, and P. Xie, 2010: Intercomparison of daily precipitation statistics over the United States in observations and in NCEP reanalysis products. *J. Climate,* **23,** 4637–4650.

Horel, J. D., A. N. Hahmann, and J. E. Geisler, 1989: An investigation of the annual cycle of convective activity over the tropical Americas. *J. Climate,* **2,** 1388–1403.

Huffman, G. J., and Coauthors, 2007: The TRMM Multisatellite Precipitation Analysis (TMPA): Quasi-global, multiyear, combined-sensor precipitation estimates at fine scales. *J. Hydrometeor.,* **8,** 38–55.

Jones, C., and L. M. V. Carvalho, 2002: Active and break phases in the South American monsoon system. *J. Climate,* **15,** 905–914.

——, ——, and B. Liebmann, 2012: Forecast skill of the South American monsoon system. *J. Climate,* **25,** 1883–1889.

Kitoh, A., S. Kusunoki, and T. Nakaegawa, 2011: Climate change projections over South America in the late 21st century with the 20 and 60 km mesh Meteorological Research Institute atmospheric general circulation model (MRI-AGCM). *J. Geophys. Res.,* **116,** D06105, doi:10.1029/2010JD014920.

Kodama, Y. M., 1992: Large-scale common features of subtropical precipitation zones (the baiu frontal zone, the SPCZ, and the SACZ). I. Characteristics of subtropical frontal zones. *J. Meteor. Soc. Japan,* **70,** 813–836.

——, 1993: Large-scale common features of subtropical convergence zones (the baiu frontal zone, the SPCZ, and the SACZ). II. Conditions of the circulations for generating the STCZS. *J. Meteor. Soc. Japan,* **71,** 581–610.

Kousky, V. E., 1988: Pentad outgoing longwave radiation climatology for the South American sector. *Rev. Bras. Meteor.,* **3,** 217–231.

Kummerow, C., W. Barnes, T. Kozu, J. Shiue, and J. Simpson, 1998: The Tropical Rainfall Measuring Mission (TRMM) sensor package. *J. Atmos. Oceanic Technol.,* **15,** 809–817.

——, and Coauthors, 2000: The status of the Tropical Rainfall Measuring Mission (TRMM) after two years in orbit. *J. Appl. Meteor.,* **39,** 1965–1982.

Lenters, J. D., and K. H. Cook, 1999: Summertime precipitation variability over South America: Role of the large-scale circulation. *Mon. Wea. Rev.,* **127,** 409–431.

Liebmann, B., and J. Marengo, 2001: Interannual variability of the rainy season and rainfall in the Brazilian Amazon basin. *J. Climate,* **14,** 4308–4318.

——, G. N. Kiladis, J. A. Marengo, T. Ambrizzi, and J. D. Glick, 1999: Submonthly convective variability over South America and the South Atlantic convergence zone. *J. Climate,* **12,** 1877–1891.

——, C. Jones, and L. M. V. Carvalho, 2001: Interannual variability of daily extreme precipitation events in the state of Sao Paulo, Brazil. *J. Climate,* **14,** 208–218.

——, G. N. Kiladis, C. S. Vera, A. C. Saulo, and L. M. V. Carvalho, 2004a: Subseasonal variations of rainfall in South America in the vicinity of the low-level jet east of the Andes and comparison to those in the South Atlantic convergence zone. *J. Climate,* **17,** 3829–3842.

——, and Coauthors, 2004b: An observed trend in central South American precipitation. *J. Climate,* **17,** 4357–4367.

——, and Coauthors, 2007: Onset and end of the rainy season in South America in observations and the ECHAM 4.5 atmospheric general circulation model. *J. Climate,* **20**, 2037–2050.

Marengo, J. A., 2004: Interdecadal variability and trends of rainfall across the Amazon basin. *Theor. Appl. Climatol.,* **78,** 79–96.

——, 2009: Long-term trends and cycles in the hydrometeorology of the Amazon basin since the late 1920s. *Hydrol. Processes,* **23,** 3236–3244.

——, B. Liebmann, V. E. Kousky, N. P. Filizola, and I. C. Wainer, 2001: Onset and end of the rainy season in the Brazilian Amazon basin. *J. Climate,* **14,** 833–852.

——, M. W. Douglas, and P. L. S. Dias, 2002: The South American low-level jet east of the Andes during the 1999 LBA-TRMM and LBA-WET AMC campaign. *J. Geophys. Res.,* **107,** 8079, doi:10.1029/2001JD001188.

——, R. Jones, L. M. Alves, and M. C. Valverde, 2009: Future change of temperature and precipitation extremes in South America as derived from the PRECIS regional climate modeling system. *Int. J. Climatol.,* **29,** 2241–2255.

——, J. Tomasella, L. M. Alves, W. R. Soares, and D. A. Rodriguez, 2011: The drought of 2010 in the context of historical droughts in the Amazon region. *Geophys. Res. Lett.,* **38,** L12703, doi:10.1029/2011GL047436.

——, and Coauthors, 2012: Recent developments on the South American monsoon system. *Int. J. Climatol.,* **32,** 1–21.

Mechoso, C. R., A. W. Robertson, C. F. Ropelewski, and A. M. Grimm, 2005: The American monsoon systems: An introduction. WMO/TD 1266 (TMRP Rep. 70), 197–206.

Moss, R. H., and Coauthors, 2010: The next generation of scenarios for climate change research and assessment. *Nature,* **463,** 747–756.

Robertson, A. W., 2000: Interannual and interdecadal variability of the South Atlantic convergence zone. *Mon. Wea. Rev.,* **128,** 2947–2957.

——, and C. R. Mechoso, 1998: Interannual and decadal cycles in river flows of southeastern South America. *J. Climate,* **11,** 2570–2581.

——, and ——, 2000: Interannual and interdecadal variability of the South Atlantic convergence zone. *Mon. Wea. Rev.,* **128,** 2947–2957.

Saha, S., and Coauthors, 2010: The NCEP Climate Forecast System reanalysis. *Bull. Amer. Meteor. Soc.,* **91,** 1015–1057.

Seth, A., M. Rojas, and S. A. Rauscher, 2010: CMIP3 projected changes in the annual cycle of the South American monsoon. *Climatic Change,* **98,** 331–357.

——, S. A. Rauscher, M. Rojas, A. Giannini, and S. J. Camargo, 2011: Enhanced spring convective barrier for monsoons in a warmer world? *Climatic Change,* **104,** 403–414.

Silva, A. E., and L. M. V. Carvalho, 2007: Large-Scale Index for South America Monsoon (LISAM). *Atmos. Sci. Lett.,* **8,** 51–57.

Silva, V. B. S., V. E. Kousky, W. Shi, and R. W. Higgins, 2007: An improved gridded historical daily precipitation analysis for Brazil. *J. Hydrometeor.,* **8,** 847–861.

——, ——, and R. W. Higgins, 2011: Daily precipitation statistics for South America: An intercomparison between NCEP reanalyses and observations. *J. Hydrometeor.,* **12,** 101–117.

Silva Dias, P. L., W. H. Schubert, and M. DeMaria, 1983: Large-scale response of the tropical atmosphere to transient convection. *J. Atmos. Sci.,* **40,** 2689–2707.

Solomon, S., D. Qin, M. Manning, Z. Chen, M. Marquis, K. Averyt, M. M. B. Tignor, and H. L. Miller Jr., Eds., 2007: *Climate Change 2007: The Physical Science Basis.* Cambridge University Press, 996 pp.

Taylor, K. E., R. J. Stouffer, and G. A. Meehl, 2012: An overview of CMIP5 and the experiment design. *Bull. Amer. Meteor. Soc.,* **93,** 485–498.

Vera, C., G. Silvestri, B. Liebmann, and P. Gonzalez, 2006a: Climate change scenarios for seasonal precipitation in South America from IPCC-AR4 models. *Geophys. Res. Lett.,* **33,** L13707, doi:10.1029/2006GL025759.

——, and Coauthors, 2006b: Toward a unified view of the American monsoon systems. *J. Climate,* **19,** 4977–5000.

Wilks, D. S., 2006: *Statistical Methods in the Atmospheric Sciences.* 2nd ed. Academic Press, 648 pp.

Zhou, J. Y., and K. M. Lau, 1998: Does a monsoon climate exist over South America? *J. Climate,* **11,** 1020–1040.